Interacting multiple model-based human motion prediction for motion planning of companion robots

Donghan Lee[1], Chang Liu[2] and J. Karl Hedrick[3]

***Abstract*— Motion planning of human-companion robots is a challenging problem and its solution has numerous applications. This paper proposes a motion planning method for human-companion robots to accompany humans in a socially desirable manner, which takes into account the safety, comfort requirements. A unified Interacting Multiple Model (IMM) framework is developed to estimate human motion states from noisy sensor data and predict human positions in a finite horizon. The robot motion planning is formulated as a model predictive control problem to generate socially desirable motion behavior based on the predicted human positions. The effectiveness of the proposed motion planning method in facilitating the socially desirable companion behavior is evaluated through simulations and the advantage of IMM framework for human motion estimation and prediction compared to traditional single model approaches has been demonstrated.**

I. INTRODUCTION

The application of autonomous robots for search-and-rescue (SAR) missions have received considerable attentions in last decades [1]–[3]. One particular interesting scenario is allowing robots to autonomously accompany humans during the SAR, assisting humans in carrying heavy apparatus, detecting signals of survivors or exploring dangerous areas.

To make the robot's companion behavior natural and amiable, referred to as being *socially desirable*, several requirements need to be satisfied, including the safety and comfort [4]. Safety serves as the fundamental guideline, requiring that robots avoid collision with accompanied humans under all circumstances [5]–[7]. Comfort requires robots to pose little annoyance and stress for the accompanied humans [4]. It is mainly formulated regarding the distance that a robot needs to keep from people. The "Proxemics" model, proposed by Hall et al. [8], has been adopted for designing robot's human-friendly motion behavior [9], [10]. This model denotes a virtual zone around a person that robots should avoiding entering in order to prevent the discomfort that the person may feel. Similarity on speed between the human and the robot has also been considered as a contributing factor for comfort [11].

To generate socially desirable motion behavior, accurate human motion prediction is necessary. To be specific, a robot needs to predict human future trajectory based on the human's motion states that are estimated from measurement of equipment such as GPS sensors or cameras. Filtering methods, such as the Kalman filter (KF) and the particle filter (PF), have been applied for tracking moving objects [12], [13], assuming certain motion pattern, such as the constant speed and direction model [7], [14]. These single-model filtering approaches can effectively predict human motion when the people follow the assumed motion pattern. However, when the human movement involves multiple models (such as making turns with changing speed), such methods may fail to give accurate prediction.

Learning techniques have also been utilized for human motion prediction in recent years. Bennewitz et al. [15] proposed a prediction approach based on the hidden Markov model, utilizing the clustered collections of trajectories that characterize typical motion patterns of persons. Fulgenzi et al. [16] developed a Gaussian process-based motion predictor, using pre-learned human motion patterns. Neural networks have also been utilized [17], [18]. These learning-based approaches have achieved success in predicting human motion in the environments where human trajectories have been previously collected for training. However, these predictors may fail to obtain accurate prediction in unknown environments that no training data is available. This drawback renders the learning-based prediction methods less applicable for SAR missions since disaster sites are diverse and rarely similar to the known ones.

In this work, we propose an Interacting Multiple Model (IMM)-based human motion prediction approach, taking advantage of the fact that human motion usually involves different motion models [19], such as straight-line movement, making turns and change of speed. Such IMM-based predictor incorporates several motion models and dynamically adjusts the mode probabilities based on the observed human trajectory. To deal with the nonlinearity of the human motion, such as making turns, Unscented Kalman Filter(UKF) is applied to each model in the IMM framework, resulting in the so-called IMM-UKF approach. Such approach can achieve higher prediction accuracy and faster response compared to single-model filtering methods such as KF and PF. Additionally, IMM-UKF does not need training and is thus applicable to unknown environments, which is advantageous over learning-based methods for SAR missions.

Utilizing the predicted human trajectory, a model predictive control (MPC)-based motion planner is developed that formulates the motion planning as a nonlinear programming, which conveniently considers the safety and comfort requirements. The MPC planner with IMM-UKF prediction

[1]Donghan Lee is with the Vehicle Dynamics & Control Lab, Department of Mechanical Engineering, University of California at Berkeley, California 94720, USA donghan.lee@berkeley.edu

[2]Chang Liu is with the Vehicle Dynamics & Control Lab, Department of Mechanical Engineering, University of California at Berkeley, California 94720, USA changliu@berkeley.edu

[3]J. Karl Hedrick is with Faculty of Mechanical Engineering, University of California at Berkeley, California 94720, USA khedrick@berkeley.edu

is evaluated using a simulated SAR scenario, in which the human rescuer moves sequentially to several destinations and the robot needs to accompany. Simulation results show that the IMM-UKF provides superior prediction performance than other methods. Using the MPC motion planner, the robot has successfully accompanied the human in a safe and comfortable manner.

The remainder of this paper is organized as follows: first, the problem of motion planning for a human-companion robot is formulated for the SAR mission; second, the IMM-UKF human state estimation and prediction method is proposed, followed by description of the MPC-based motion planner; next, simulation setup and results on evaluating the proposed approach are presented; lastly, concluding remarks and ideas of future work are presented.

II. PROBLEM FORMULATION

Consider the SAR scenario (Fig. 1) in which a human first responder needs to deliver medical treatment to several destinations that contain injured people. A companion robot that carries medical apparatus will accompany the human and sequentially move to these destinations. The robot has no knowledge about the positions of human destinations. However, it can measure human positions in real time from the GPS sensor that the human carries.

Several obstacles exist in the field, including five stationary ones (blue rectangles), representing unmovable obstructions such as buildings or plants, and two moving ones (pink dots with arrows showing moving direction) representing mobile objects such as pedestrians or vehicles. The positions of stationary obstacles are known to both the human and the companion robot while the moving obstacles are measured using same measurement tool for tracking the human rescuer. When accompanying the human, the robot should satisfy the aforementioned safety and comfort requirements, illustrated in Fig. 2. To be specific, a circular "safety zone" with radius d_s is defined around the target person. Stepping into the"safety zone" is considered as unsafe behavior and thus should be strictly prohibited. The comfort requires the robot to stay within a "comfort range" of distance from the human and also keep similar speed. Unlike the safety requirement, the violation of comfort is acceptable, though not desirable.

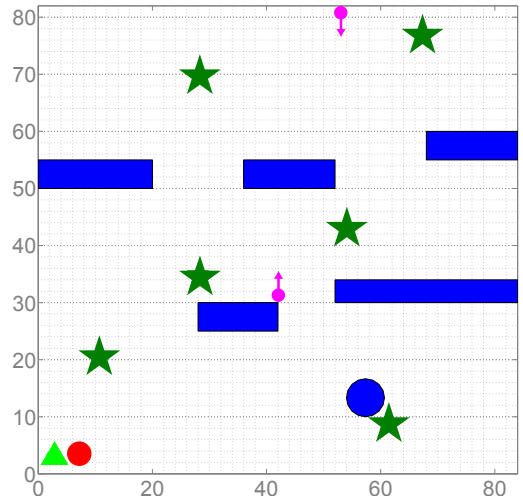

Fig. 1: A search-and-rescue scenario for the companion robot to accompany a human. The red circle and the green triangle represent the human rescuer and the robot companion, respectively. Stars denote human destinations and the blue rectangles stand for static obstacles. Moving obstacles are shown as pink circles with arrows.

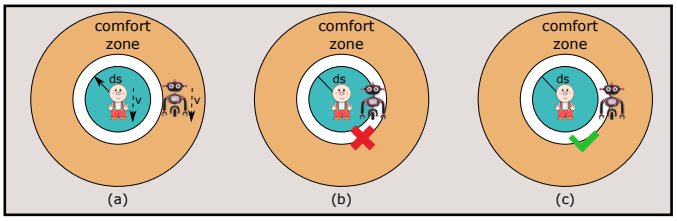

Fig. 2: Illustration of safety and comfort requirements. The blue circle represents the "safety zone" and the orange area represents the "comfort range". (a) The most desirable companion behavior is that the robot stays within the "comfort range" and maintains similar speed as the human. (b) The robot is not allowed to enter the "safety zone". (c) It is acceptable, but not desirable, that the robot stays outside of the "comfort range" and the "safety zone".

III. METHODS

A. Human Motion Estimation and Prediction

1) Interacting Multiple Model: The Interacting Multiple Model (IMM) approach are applied for estimating the human motion from the noisy sensor data. It utilizes a bank of r number of filters corresponding to different motion models. State estimate at time k is computed as a weighted sum of estimates from each filter, as shown in the following formula:

$$\hat{x}(k|k) = \sum_{j=1}^{r} \mu_j(k)\hat{x}^j(k|k) \tag{1}$$

where r denotes the number of models; $\hat{x}^j(k|k)$ represents the state estimate from the j^{th} filter; $\mu_j(k)$ stands for the mode probability and is computed as follows:

$$\mu_j(k) = \frac{1}{c}\sum_{i=1}^{r} L_{ij}(k)p_{ij}\mu_j(k-1)$$

where c denotes the normalizing factor; $L_{ij}(k)$ stands for the Gaussian likelihood of receiving the current measurement given all previous measurements and that model j is in effect at time k and p_{ij} represents the mode transition probability from the i^{th} to the j^{th} model. Each filter uses the mixed initial state estimate and covariance from an interaction of the r filters, which consists of the mixing of the estimates with the mixing probability at previous time step. Readers interested in the details of the IMM approach can refer to [20].

In this work, two different dynamic models are used in the IMM framework: one is the coordinated turn motion

model, reflecting the action of making turns or moving along a curved path, and the other is the uniform motion model, representing the straight-line movement. The equation for the coordinated turn motion is shown below:

$$x^{h,1}(k+1) = f(x^{h,1}(k)) + Gw_1(k)$$

$$f(x^{h,1}(k)) = \begin{bmatrix} p_1^h + \frac{\sin(\omega^h T)}{\omega^h} v_1^h - \frac{1-\cos(\omega^h T)}{\omega^h} v_2^h \\ \cos(\omega^h T) v_1^h - \sin(\omega^h T) v_2^h \\ p_2^h + \frac{1-\cos(\omega^h T)}{\omega^h} v_1^h + \frac{\sin(\omega^h T)}{\omega^h} v_2^h \\ \sin(\omega^h T) v_1^h + \cos(\omega^h T) v_2^h \\ \omega^h \end{bmatrix}$$

$$G = \begin{bmatrix} \frac{T^2}{2} & 0 & 0 \\ T & 0 & 0 \\ 0 & \frac{T^2}{2} & 0 \\ 0 & T & 0 \\ 0 & 0 & 1 \end{bmatrix}$$

$$w_1 \sim \mathcal{N}(0, Q).$$

Also, the equation of the uniform motion is represent as follows:

$$\dot{x}^{h,2}(k+1) = Ax^{h,2}(k) + Bw_2(k)$$

$$A = \begin{bmatrix} 1 & T & 0 & 0 & 0 \\ 0 & 1 & 0 & 0 & 0 \\ 0 & 0 & 1 & T & 0 \\ 0 & 0 & 0 & 1 & 0 \\ 0 & 0 & 0 & 0 & 0 \end{bmatrix}, \; B = \begin{bmatrix} \frac{T^2}{2} & 0 & 0 \\ T & 0 & 0 \\ 0 & \frac{T^2}{2} & 0 \\ 0 & T & 0 \\ 0 & 0 & 1 \end{bmatrix}$$

$$w_2 \sim \mathcal{N}(0, Q)$$

where $x^{h,i}(k)$, $i = 1, 2$ represents the human motion state including five elements : $p_1^h, v_1^h, p_2^h, v_2^h, \omega^h$, where p_1^h, p_2^h denote the longitudinal and lateral position of the human, v_1^h, v_2^h the corresponding velocity and ω^h the turn rate of the human; $w_i(k)$, $i = 1, 2$ represents process noise; T represents the sampling time; Q is the covariance matrix of the process noise.

The uniform motion model is essentially a special case of the coordinated turn motion model with the turn rate ω being fixed to zero. However, including two models are necessary since this allows the estimator for fast detection of change of motions. It seems that only considering the coordinated turn motion model suffices to estimate human motion states, in addition to the benefits of reduced computations by using the single model. However, including two models are necessary since this allows the estimator for fast detection of change of motions. In other words, it is common to include one uniform motion model and one coordinated turn motion model for quick motion-change detection. Since human motion usually involves different motions in the real world, the ability to quickly detect the change of the motion is one of the important properties for the estimation and prediction.

The observation equation is represented as :

$$y^h(k) = Cx^h(k) + v(k) \tag{2}$$

where $y^h(k)$ denotes the observed human state at the time step k; $v(k)$ stands for measurement noise.

By using GPS sensors, the human positions can be measured. Therefore, the parameters in observation model Eq. (2) is defined as:

$$C = \begin{bmatrix} 1 & 0 & 0 & 0 \\ 0 & 0 & 1 & 0 \end{bmatrix}, \tag{3a}$$

$$v \sim \mathcal{N}(0, V) \tag{3b}$$

where V is the convariance matrix of the measurement noise. The above two models are utilized for human motion state estimation, in combination with the Unscented Kalman Filter.

2) Unscented Kalman Filter: The Unscented Kalman Filter (UKF) is applied to each model that are used in IMM framework for estimating human states. It is an effective state estimation technique for nonlinear systems by implementing the Unscented Transformation (UT) that calculates the statistics of a random vector that undergoes a nonlinear transformation [21]. To be specific, given an arbitrary nonlinear dynamic model $z = g(x)$ and as L-dimensional Gaussian Random Vector (GRV) x with mean $\hat{x}$ and covariance P_x, the statistics of z can be approximated by using $2L+1$ discrete sample points $\{\chi^{(i)}\}_{i=0}^{2L} = \{\hat{x} \text{ and } \hat{x} \pm \sigma_j, j = 1, ..., L\}$, called *sigma points*, where σ_j is the j^{th} column of the matrix $\sqrt{(L+\lambda)P_x}$. λ is a scaling parameter, as defined below:

$$\lambda = \alpha^2(L + \kappa) - L \tag{4a}$$

$$W_0^{(m)} = \frac{\lambda}{L+\lambda} \tag{4b}$$

$$W_0^{(c)} = \frac{\lambda}{L+\lambda} + 1 - \alpha^2 + \beta \tag{4c}$$

$$W_i^{(m)} = W_i^{(c)} = \frac{1}{L+\lambda}, \quad i = 1, ..., 2L \tag{4d}$$

where α determines the spread of sigma points about the mean $\hat{x}$; κ is a secondary scaling parameter; β is used to incorporate prior knowledge of the distribution.

Once the sigma points have been generated, each point is passed through the nonlinear function $z = g(x)$, i.e. each column of the sigma points is propagated through the nonlinearity, as in $\zeta^{(i)} = g(\chi^{(i)}), i = 0, ..., 2L$. The mean $\hat{z}$ and the covariance P_z are approximated as $\hat{z} \simeq \Sigma_{i=0}^{2L} W_i^{(m)} \zeta^{(i)}$ and $P_z \simeq \Sigma_{i=0}^{2L} W_i^{(c)} (\zeta^{(i)} - \hat{z})(\zeta^{(i)} - \hat{z})^\mathsf{T}$, calculated as given in above equations of the weights and parameters [22]. The state estimate, $\hat{x}^j(k|k)$, $j = 1, ..., r$ in Eq. (1), can be computed like $\hat{z}$ at each filter that have different dynamics models. Readers can refer to [21] for more details of the UKF algorithm.

3) Human Motion Prediction: The estimated human motion states and the mode probabilities are utilized for predicting human future states. To be specific, using the uniform motion model and the turn motion model, human positions for each model can be extrapolated and then combined based on the mode probabilities to obtain the predicted positions. Let $\hat{x}^{h,j}(k|k)$ and $\tilde{x}^{h,j}(k+i|k)$ represent the estimated and predicted human states associated with the j^{th} model at time k and $k+i$ $(i \geq 0)$, respectively, based on the observations

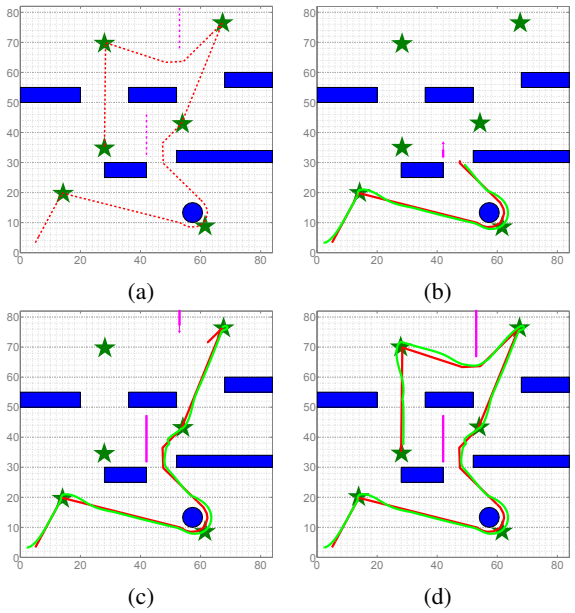

Fig. 3: A screenshot of the simulation. The red line represents the human trajectory and the green on shows the companion robot's trajectory. For most of the time, the robot follows the human from behind

up to time k. The prediction procedure works as follows:

$$\tilde{x}^h(k+l+1|k) = \sum_{j=1}^{r} \mu_j \tilde{x}^{h,j}(k+l+1|k) \tag{5a}$$

$$l = 0, \ldots, N-1$$

$$\tilde{x}^{h,j}(k+l+1|k) = \Sigma_{i=0}^{2L} W_i^{(m)} \chi_{k+l+1|k}^{(i)} \tag{5b}$$

$$j = 1, \ldots, r$$

$$\chi_{k+l+1|k}^{(i)} = f(\chi_{k+l|k}^{(i)}) \quad i = 0, \ldots, 2L \tag{5c}$$

$$\chi_{k|k}^{(i)} = \left[\hat{x}^{h,j}(k|k) \;\; \hat{x}^{h,j}(k|k) \pm \sigma_m^{h,j}(k|k)\right] \tag{5d}$$

$$\sigma_m^{h,j}(k|k) = \sqrt{(L+\lambda) P_x^{h,j}(k|k)} \quad m = 1, \ldots, L \tag{5e}$$

where N denotes the prediction horizon; r represents the number of models; L is the dimension of $x^{h,j}$; $P_x^{h,j}$ stands for the covariance associated with the j^{th} model at time k; λ is represented in Eq. (4a).

B. Robot motion Planning

The model predictive control (MPC) approach is utilized for robot motion planning. It iteratively solves a finite-horizon constrained optimal control problem: after computing the optimal control inputs over the planning horizon, it implements the first input and then computes for a new set of control inputs, starting from the updated state. Let $p^h(k) = \begin{bmatrix} p_1^h(k) \\ p_2^h(k) \end{bmatrix}$ and $v^h(k) = \left\| \begin{bmatrix} v_1^h(k) \\ v_2^h(k) \end{bmatrix} \right\|_2$ represent the position vector and the speed of the human at time k, respectively. Notations for the estimated and predicted position vector and speed can be defined as $\hat{p}^h(k|k), \tilde{p}^h(k+i|k), \hat{v}^h(k|k), \tilde{v}^h(k+i|k)$, respectively. The optimal control inputs are obtained by solving the following nonlinear programming problem that incorporates the kinematics of the robot and the safety and comfort requirements:

$$\min_{\mathbf{A}_k, \mathbf{\Theta}_k} \quad \sum_{i=1}^{N} q_1 \left| \left\| \bar{p}^r(k+i|k) - \tilde{p}^h(k+i|k) \right\|_2^2 - d_c^2 \right| + q_2 \left| \bar{v}^r(k+i|k) - \tilde{v}^h(k+i|k) \right|^2 \tag{6a}$$

$$\text{s.t.} \quad \bar{p}^r(k+i|k) = \bar{p}^r(k+i-1|k) + \bar{v}^r(k+i-1|k) \begin{bmatrix} \cos\theta(k) \\ \sin\theta(k) \end{bmatrix} T \tag{6b}$$

$$v^r(k+i|k) = v^r(k+i-1|k) + a(k+i-1|k)T \tag{6c}$$

$$\theta^r(k+i|k) = \theta^r(k+i-1|k) + w(k+i-1|k)T \tag{6d}$$

$$a_{lb} \le a^r(k) \le a_{ub} \tag{6e}$$

$$w_{lb} \le \omega^r(k) \le w_{ub} \tag{6f}$$

$$||\bar{p}^r(k+i|k) - \tilde{p}^h(k+i|k)||_2 > d_s \tag{6g}$$

$$||\bar{p}^r(k+i|k) - \tilde{p}_{l_m}^{obs_m}(k+i|k)||_2 > d_s \tag{6h}$$

$$l_m = 1, \ldots, n_m$$

$$h_{l_s}(\bar{p}^r(k+i|k)) \ge 0 \tag{6i}$$

$$h_{l_s}(\lambda \bar{p}^r(k+i-1|k) + (1-\lambda)\bar{p}^r(k+i|k)) \ge 0 \tag{6j}$$

$$\forall l_s = 1, \ldots, n_s, \; 0 \le \lambda \le 1$$

$$\bar{p}^r(k|k) = p^r(k) \tag{6k}$$

$$\bar{v}^r(k|k) = v^r(k) \tag{6l}$$

$$\bar{\theta}^r(k|k) = \theta^r(k) \tag{6m}$$

where $\bar{p}^r(k+i|k)$, $\bar{v}^r(k+i|k)$ and $\bar{\theta}(k+i|k)$, $1 \le i \le N$ represent the planned position, speed and heading angle at time $k+i$, respectively; N is the prediction horizon; n_m stands for the number of moving obstacles and $p_{l_m}^{obs_m}$ denotes the position of the l_m-th moving obstacle; n_s is the number of static obstacles. These static obstacles are approximated by ellipsis, the details of which are described in the Appendix-B. $h_{l_s}(\cdot)$ denotes the analytical function of the ellipse approximation of the l_s-th static obstacle. $(\mathbf{A}_k, \mathbf{\Theta}_k)$ stand for the set of optimal acceleration and angular velocity in the prediction horizon $[k, k+N-1]$, obtained by solving the above optimization problem at time k.

The objective function Eq. (6a) consists of two terms: the first one stands for the difference between the squared human-robot distances and the squared comfort distance; the second one represents the speed difference between the robot and the human. This reflects the comfort requirement that the robot maintain the comfort distance from the human and keep similar pace at the same time. q_1 and q_2 denote the weights for these two terms.

The safety constraints are imposed in Eqs. (6g) to (6j). Eqs. (6g) and (6h) regulates that the robot stay at least the safety distance d_s from the human and moving obstacles in order to avoid collision. To predict moving obstacles, the

same motion prediction method described in Section III-A.3 is applied. Eqs. (6i) and (6j) enforce the collision avoidance with static obstacles. To be specific, Eq. (6i) demands that each way point of the robot be kept outside of static obstacles and Eq. (6j) requires that the trajectory connecting the adjacent waypoints not intersect with obstacles, which eliminates the path that leads the robot across obstacles. Eqs. (6k) to (6m) initializes the robot's planned states based on its actual state at time k.

IV. SIMULATION RESULTS & DISCUSSION

A. Simulation setup

Simulations have been run to evaluate the proposed MPC planner with IMM-UKF for prediction. A human rescuer will move sequentially to six targets with constant speed of $1.5m/s$ in a $84m \times 82m$ field, following the trajectory as shown in Fig. 3a. Notice that such trajectory covers several typical human motion patterns, including straight-line movement, motion following curved paths and making sharp turns. Therefore, it provides a realistic testbed for evaluating the proposed MPC planner with IMM-UKF for prediction. Both the trajectory and human speed are unrevealed to the robot. The safety distance d_s is chosen as $1m$. According to the research by Hall et al. [8], the comfort distance range is from 1.2m to 3.6m. In the simulation, we choose d_c as $2.4m$, which is the median value of the comfort range. However, any distance within $[1.2m, 3.6m]$ is considered a comfortable one. The sampling rate of GPS sensor is $20Hz$ and the variance of sensor measurement noise is considered as $2m$. The robot's maximum acceleration and deceleration are set to be $1m/s^2$ and $-3m/s^2$ respectively and the angular velocity range is chosen to be $[-90°/s, 90°/s]$. In the IMM estimator, the process noise and the measurement noise are set to be 1.5×10^{-2} and 1.5, respectively. The parameters of UKF in the estimator are $L = 5, \alpha = 0.001, \kappa = 0$ and $\beta = 2$. The prediction horizon for the human motion is chosen as $2.5s$ and the robot iteratively computes the control inputs every $500ms$.

B. Simulation results

Figs. 3a to 3d show both the human and robot's trajectories. The performance of human motion estimation and prediction is evaluated by comparing with three other filtering methods. The MPC-based robot motion planning method is then evaluated under different prediction strategies.

1) Human motion estimation: The error between the estimated and the actual human position and speed at each time step are compared to evaluate the estimation accuracy. The position error vector can be formulated as:

$$\Delta_p^{est}(k) = p^h(k) - \hat{p}^h(k|k)$$

where $p^h(k)$ denotes the actual human position at time k.

Fig. 4 shows the position estimation error on longitudinal and lateral directions using four different estimators: Linear Kalman Filter (LKF), IMM-LKF, UKF and IMM-UKF. In the simulation, the same turn motion model in IMM-UKF is adopted for the system dynamics in UKF; the uniform

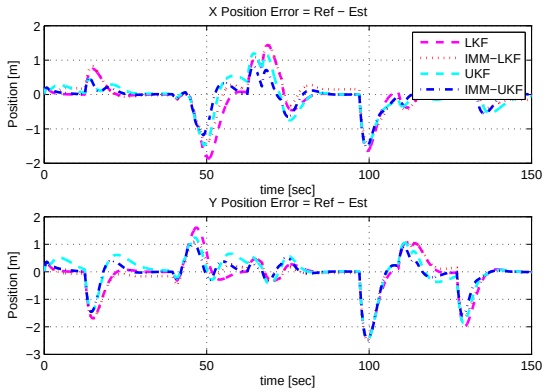

Fig. 4: Comparison of position estimation error with LKF, IMM-LKF, UKF and IMM-UKF

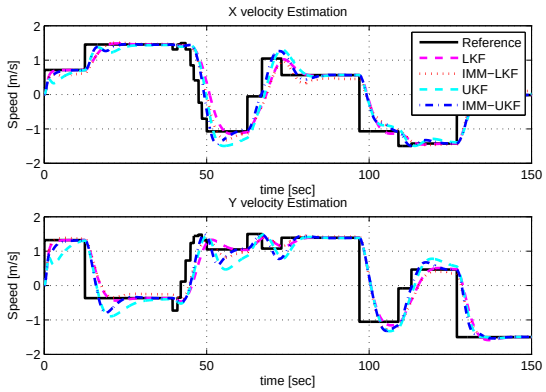

Fig. 5: Comparison of the estimated velocity using the IMM-based and the single-model approaches

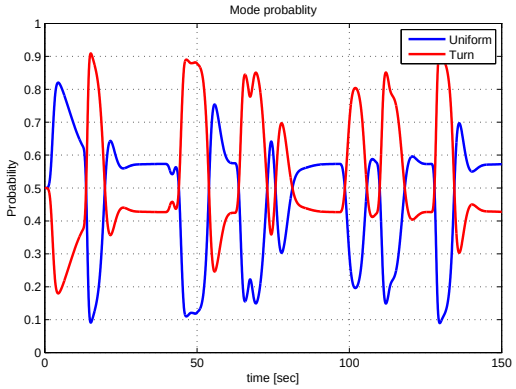

Fig. 6: Model probabilities of two models in the IMM-UKF estimator

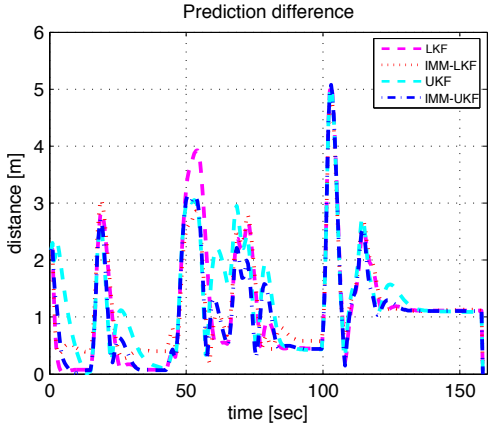

Fig. 7: Comparison of prediction error between the IMM-based and single-model approaches

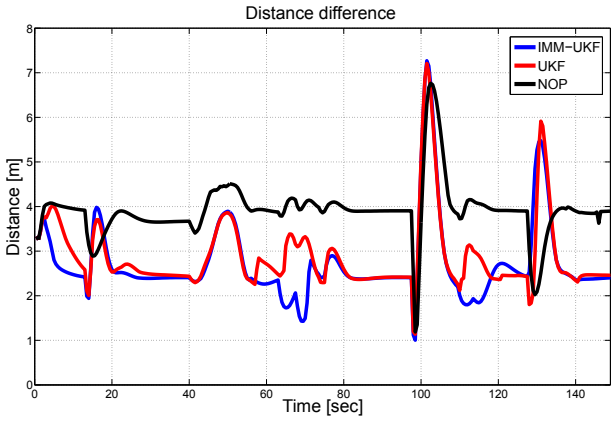

Fig. 8: Comparison of distance between the human and the robot using the MPC and the reactive methods

motion model in IMM-LKF is also applied as the dynamic model in LKF. Several observations can be obtained in this figure. First, the responses of the nonlinear estimators such as UKF and IMM-UKF are faster than the linear estimators. Second, the IMM-based approaches show better performance in accuracy than the single-model approaches. Besides, IMM-UKF achieves the fastest response and best accuracy compared to other methods, especially when the human turns around the circular obstacle at time 50. Fig. 5 compares the velocity estimation using four estimators. Overall, the nonlinear estimators (UKF and IMM-UKF) show faster response compared to the linear estimators (LKF and IMM-LKF), though they have overshoots due to the fast response. It is worth noting that the overshoots of IMM-UKF are smaller than UKF while keeping the fast response at time 53 and 118 when the velocity changes abruptly. This makes sense as the IMM-UKF estimator incorporates uniform motion model that can capture the sudden velocity changes. Fig. 6 shows the mode probabilities of the uniform motion model and turn motion model in IMM-UKF over time. When the human speed changes, the mode probability of the turn motion becomes higher than that of the uniform motion. These changes illustrates the reason that IMM-based estimators achieve more accurate and faster estimation than the single-model estimator at the sharp turn and circular turn, thus demonstrating the necessity of applying IMM-UKF estimator for human tracking.

2) Human motion prediction: To evaluate the IMM-UKF prediction, the average prediction error over the prediction horizon is computed and compared with the LKF, IMM-LKF and UKF. At time k, the prediction error is defined as:

$$\Delta_p^{pre}(k) = \frac{1}{N}\sum_{i=1}^{N} ||\tilde{p}^h(k+i|k) - p^h(k+i)||_2 \qquad (7)$$

Different from the IMM-based prediction approaches that extrapolate the human position by a weighted sum of the predicted positions from each model, the single-model methods only utilize one of the motion models for prediction.

Fig. 7 shows the comparison of prediction error using two single-model approaches (LKF, UKF) and two IMM-based methods (IMM-LKF, IMM-UKF). It can be noticed that single-model approaches generate larger prediction error than IMM-based methods, especially when the human makes turns, such as at time 50. This makes sense as IMM-based methods have already considered both uniform and turn motion models. Based on the simulation results, IMM-UKF is shown to outperform the other three prediction approaches.

3) Robot motion planning: Fig. 3d shows the trajectory of the companion robot that accompanies the target person moving in the field. The trajectory is generated by the proposed MPC motion planner with five-step planning horizon ($2.5s$) and using the IMM-UKF for predicting the human and moving obstacles' trajectories. The performance of the motion planning is evaluated using the criterion of safety and comfort. To be specific, the distance and speed differences between the robot and the human at each time step are measured, which are defined as:

$$\Delta_d(k) = ||p^r(k) - p^h(k)||_2 \qquad (8a)$$

$$\Delta_v(k) = |v^r(k) - v^h(k)| \qquad (8b)$$

These quantities are illustrated as the blue line in Figs. 8 and 9.

The performance of IMM-UKF is compared with two benchmark prediction strategies, using the same MPC planner. The first benchmark method uses the coordinate turn motion model and applies UKF to predict human motion. The second method does not predict human motion. Instead, the robot only utilize the human's current state for one-step ($500ms$) motion planning.

Fig. 8 compares the distances between the human and the robot using these three strategies. It can be noticed that the MPC planner has ensured the safety of the accompanied human with each of the three prediction methods in that no distance goes below d_s. Additionally, by incorporating human motion prediction into the motion planning, the robot significantly improves its companion performance from the non-prediction case. In fact, the average distance between the human and the robot are 2.716, 2.8774, 3.8913 using the

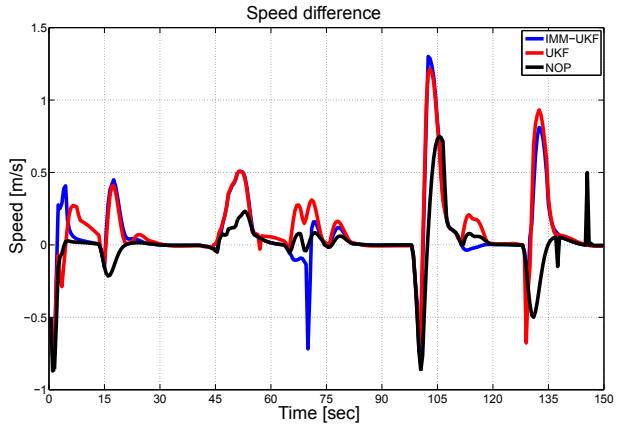

Fig. 9: Comparison of velocity difference between the human and the robot using the MPC and the reactive methods

IMM-UKF, UKF and non-prediction methods respectively. Besides, the IMM-UKF achieves better performance than the UKF in that the average distance is smaller but still within the comfort range using the IMM-UKF.

The non-prediction method achieves smaller speed difference than methods using prediction. This seems to imply that the non-prediction method is preferable for the robot to keep similar pace as the human. However, such speed similarity using non-prediction method results in large distance between the human and the robot, which is undesirable. The change of the speed when using prediction is caused by the motion planner's effort to keep the robot within the comfort region around the human. Therefore, the simulation results show the superiority of using the IMM-UKF prediction for robot motion planning.

V. CONCLUSION

We have developed an autonomous motion planning framework for human-companion robots to accompany a target person in a socially desirable manner. Such companion robot can be useful for search-and-rescue scenarios by assisting humans in carrying apparatus, exploring dangerous areas or detecting survivors. The IMM-UKF approach that incorporates the uniform motion model and the coordinated turn motion models is proposed for human motion estimation and prediction. Such multiple-model approach captures different human motion patterns, thus improving the estimation and prediction accuracy than other three approaches: LKF, IMM-LKF and UKF. Based on the predicted human position and speed, the model predictive control (MPC) approach is utilized for planning robot trajectory, which considers the safety and comfort of the behavior. Simulation results show superior performance in terms of the accuracy and response time in the estimation and prediction using the IMM-UKF approach, especially when the human makes curved motion or sharp turns. Moreover, the MPC planner is evaluated using the IMM-UKF, the UKF and non-prediction methods. The planner successfully ensures the safety of the accompanied person using all these prediction strategies. The IMM-UKF results in best robot motion behavior by keeping the robot within the comfort distance range from the human.

In the future work, we plan to investigate other motion prediction methods, such as the auto-regressive moving-average (ARMA) method, and compare with IMM-UKF method. Besides, enabling the robot to learn human motion model in real time is an attractive topic and may provide more accurate human motion prediction and results in better human-companion behavior.

APPENDIX

A. IMM-LKF Method

Similar to IMM-UKF, IMM-LKF works with two dynamic models: one is the uniform motion model; the other is the coordinated turn motion model. If the turn rate is a known constant in the coordinated turn motion model in **??**, the human estimation procedure can be modeled with the discrete time linear state space system as follows:

$$x^h(k+1) = Ax^h(k) + B_w w(k) \tag{9a}$$

$$y^h(k) = Cx^h(k) + v(k) \tag{9b}$$

where $x^h(k)$ and $y^h(k)$ represent the human motion state and the observation, respectively, at the time step k; $w(k)$ and $v(k)$ represent process noise and measurement noise, respectively. $x^h(k)$ consists of four elements: $p_1^h, v_1^h, p_2^h, v_2^h$, where p_1^h, p_2^h denote the longitudinal and lateral position of the human and v_1^h, v_2^h the corresponding velocity. We use two Linear Kalman Filters in the IMM for human tracking, each corresponding to a different dynamic model: the uniform motion model and the turn motion model. Two models differ in the A matrix and w in Eq. (9a) while sharing the same B_w. In particular, we define the matrices as follows:

$$A_U = \begin{bmatrix} 1 & T & 0 & 0 \\ 0 & 1 & 0 & 0 \\ 0 & 0 & 1 & T \\ 0 & 0 & 0 & 1 \end{bmatrix},$$

$$A_T = \begin{bmatrix} 1 & \frac{\sin(\omega T)}{\omega} & 0 & \frac{1-\cos(\omega T)}{\omega} \\ 0 & \cos(\omega T) & 0 & -\sin(\omega T) \\ 0 & \frac{1-\cos(\omega T)}{\omega} & 1 & \frac{\sin(\omega T)}{\omega} \\ 0 & \sin(\omega T) & 0 & \cos(\omega T) \end{bmatrix},$$

$$B_w = \begin{bmatrix} \frac{T^2}{2} & T & 0 & 0 \\ 0 & 0 & \frac{T^2}{2} & T \end{bmatrix},$$

$$w_U \sim \mathcal{N}(0, Q_U)\ w_T \sim \mathcal{N}(0, Q_T)$$

where A_U and A_T stand for the A matrices of the uniform motion model and turn motion model, respectively; w_U and w_T denote the process noise of the uniform motion model and turn motion model, respectively; T represents the sampling time; ω represents the constant turn rate.

We assume that only the human position can be measured. Therefore, the parameters in observation model Eq. (9b) can be defined as:

$$C = \begin{bmatrix} 1 & 0 & 0 & 0 \\ 0 & 0 & 1 & 0 \end{bmatrix},$$

$$v \sim \mathcal{N}(0, V)$$

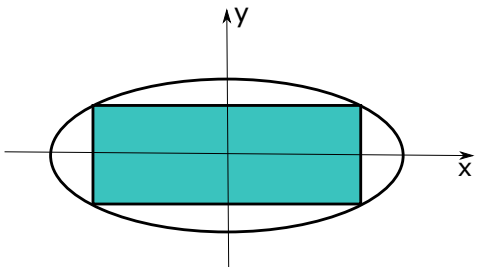

Fig. 10: Approximating the rectangle obstacle with an ellipse.

Above linear state space models are used in LKF and IMM-LKF in this paper. Moreover, we set the turn rate ω to be 0.1 rad/s as a known constant, in the turn motion model in IMM-LKF.

B. Approximating Static Obstacles

Static rectangular obstacles are approximated and analytically represented as ellipses, as shown in Fig. 10. Let a and b be the length and width of a rectangular obstacle centered at the origin. Let Eq. (12) represent the ellipse that encloses the obstacle in the way that the four vertices of the rectangle lie on the boundary of the ellipse:

$$\frac{x^2}{\alpha^2} + \frac{y^2}{\beta^2} = 1 \tag{12}$$

In addition, assume that the rectangle and ellipse have the same aspect ratio, which means $\frac{a}{b} = \frac{\alpha}{\beta}$, then by simple algebraic manipulation, we can obtain that $\alpha = \frac{a}{\sqrt{2}}$ and $\beta = \frac{b}{\sqrt{2}}$. Define

$$h(x, y) = 2\frac{x^2}{a^2} + 2\frac{y^2}{b^2} - 1.$$

Then $h(x, y) = 0$ represent the ellipse approximation of the rectangle with length a and width b. Any point (x, y) with $h(x, y) > 0$ lies outside of the ellipse.

REFERENCES

[1] J. Casper and R. R. Murphy, "Human-robot interactions during the robot-assisted urban search and rescue response at the world trade center," *Systems, Man, and Cybernetics, Part B: Cybernetics, IEEE Transactions on*, vol. 33, no. 3, pp. 367–385, 2003.

[2] I. R. Nourbakhsh, K. Sycara, M. Koes, M. Yong, M. Lewis, and S. Burion, "Human-robot teaming for search and rescue," *Pervasive Computing, IEEE*, vol. 4, no. 1, pp. 72–79, 2005.

[3] G.-J. M. Kruijff, F. Colas, T. Svoboda, J. Van Diggelen, P. Balmer, F. Pirri, and R. Worst, "Designing intelligent robots for human-robot teaming in urban search and rescue.," in *AAAI Spring Symposium: Designing Intelligent Robots*, 2012.

[4] T. Kruse, A. K. Pandey, R. Alami, and A. Kirsch, "Human-aware robot navigation: A survey," *Robotics and Autonomous Systems*, vol. 61, no. 12, pp. 1726–1743, 2013.

[5] F. Hoeller, D. Schulz, M. Moors, and F. E. Schneider, "Accompanying persons with a mobile robot using motion prediction and probabilistic roadmaps," in *Intelligent Robots and Systems, 2007. IROS 2007. IEEE/RSJ International Conference on*, pp. 1260–1265, IEEE, 2007.

[6] D. Fox, W. Burgard, S. Thrun, *et al.*, "The dynamic window approach to collision avoidance," *IEEE Robotics & Automation Magazine*, vol. 4, no. 1, pp. 23–33, 1997.

[7] M. Svenstrup, T. Bak, and H. J. Andersen, "Trajectory planning for robots in dynamic human environments," in *Intelligent Robots and Systems (IROS), 2010 IEEE/RSJ International Conference on*, pp. 4293–4298, IEEE, 2010.

[8] E. T. Hall, R. L. Birdwhistell, B. Bock, P. Bohannan, A. R. Diebold Jr, M. Durbin, M. S. Edmonson, J. Fischer, D. Hymes, S. T. Kimball, *et al.*, "Proxemics [and comments and replies]," *Current anthropology*, pp. 83–108, 1968.

[9] M.-L. Barnaud, N. Morgado, R. Palluel-Germain, J. Diard, and A. Spalanzani, "Proxemics models for human-aware navigation in robotics: Grounding interaction and personal space models in experimental data from psychology," in *Proceedings of the 3rd IROS2014 workshop Assistance and Service Robotics in a Human Environment*, 2014.

[10] J. Rios-Martinez, A. Renzaglia, A. Spalanzani, A. Martinelli, and C. Laugier, "Navigating between people: A stochastic optimization approach," in *Robotics and Automation (ICRA), 2012 IEEE International Conference on*, pp. 2880–2885, IEEE, 2012.

[11] P. Henry, C. Vollmer, B. Ferris, and D. Fox, "Learning to navigate through crowded environments," in *Robotics and Automation (ICRA), 2010 IEEE International Conference on*, pp. 981–986, IEEE, 2010.

[12] D. Koller, J. Weber, and J. Malik, *Robust multiple car tracking with occlusion reasoning*. Springer, 1994.

[13] Y. Rui and Y. Chen, "Better proposal distributions: Object tracking using unscented particle filter," in *Computer Vision and Pattern Recognition, 2001. CVPR 2001. Proceedings of the 2001 IEEE Computer Society Conference on*, vol. 2, pp. II–786, IEEE, 2001.

[14] A. Bruce and G. Gordon, "Better motion prediction for people-tracking," in *Proc. of the Int. Conf. on Robotics & Automation (ICRA), Barcelona, Spain*, 2004.

[15] M. Bennewitz, W. Burgard, G. Cielniak, and S. Thrun, "Learning motion patterns of people for compliant robot motion," *The International Journal of Robotics Research*, vol. 24, no. 1, pp. 31–48, 2005.

[16] C. Fulgenzi, C. Tay, A. Spalanzani, and C. Laugier, "Probabilistic navigation in dynamic environment using rapidly-exploring random trees and gaussian processes," in *Intelligent Robots and Systems, 2008. IROS 2008. IEEE/RSJ International Conference on*, pp. 1056–1062, IEEE, 2008.

[17] A. F. Foka and P. E. Trahanias, "Probabilistic autonomous robot navigation in dynamic environments with human motion prediction," *International Journal of Social Robotics*, vol. 2, no. 1, pp. 79–94, 2010.

[18] Z. Wu, M. Hashimoto, B. Guo, and K. Takahashi, "A path prediction method for human-accompanying mobile robot based on neural network," in *Intelligent Science and Intelligent Data Engineering*, pp. 35–42, Springer, 2012.

[19] J. K. Aggarwal and Q. Cai, "Human motion analysis: A review," *Computer vision and image understanding*, vol. 73, no. 3, pp. 428–440, 1999.

[20] B.-S. Yaakov, X. Li, and K. Thiagalingam, "Estimation with applications to tracking and navigation," *New York: Johh Wiley and Sons*, vol. 245, 2001.

[21] S. Haykin, *Kalman filtering and neural networks*, vol. 47. John Wiley & Sons, 2004.

[22] S. Hong, T. Smith, F. Borrelli, and J. K. Hedrick, "Vehicle inertial parameter identification using extended and unscented kalman filters," in *Intelligent Transportation Systems-(ITSC), 2013 16th International IEEE Conference on*, pp. 1436–1441, IEEE, 2013.